Bayesian Data-Analysis Toolbox
Release 4.23, Manual Version 3

G. Larry Bretthorst
Biomedical MR Laboratory
Washington University School Of Medicine,
Campus Box 8227
Room 2313, East Bldg.,
4525 Scott Ave.
St. Louis MO 63110
http://bayes.wustl.edu
Email: gbretthorst@wustl.edu

September 18, 2018

Chapter 27

Phasing An Image Using Non-Linear Phases

The phasing algorithm presented in Chapter 26 can phase any NMR image in which the phases vary linearly in both domains. Consequently that phasing algorithm works well for spin echo and EPI images, but it does not work for gradient echos because in gradient echos the phase varies non-linearly. This effect is illustrated in Fig. 27.1 panels (A) and (B). The linear phasing algorithm has removed most of the oscillations, but has left behind a slowly varying phase that causes the signal to oscillate between the real and imaginary channels. In Panel (C) and (D) we have displayed the real and imaginary images after the nonlinear phasing routine has been run. The nonlinear phasing routine has moved all of the image from the imaginary changes into the real channel and left behind what appears to be white noise. Indeed if you compute the standard deviation of the noise from a region that contains no signal in the real and imaginary images, you will find they are nearly identical. In this chapter we describe the interface to the nonlinear phasing package, BayesPhase2, and give the calculations needed to phase a gradient echo.

27.1 The Model Equation

As in all Bayesian calculations, the calculations begin by relating the parameters of interest to the data, i.e., by stating the model. The model we are going to use is a pixel model. That is to say, we will use exactly the same model on every pixel and each pixel will be treated independently of ever other pixel. Because each pixel is being treated separately, if the image is 128 by 256 then there are a total of 32K different calculations that must be performed. However, each calculation involves only one complex data and two parameters so the calculations are very fast.

Because the discrete Fourier transform is an information preserving transformation, it does not mater if we do the calculation in the time or image domain; both calculations are equivalent. For convenience we will present this calculation in the image domain. What we wish to do is to determine how uncertain we are of both the phase and the amplitude in each pixel and then use the phase to generate a phased image. In a real sense we are not interested in either the amplitude and phase, rather we are interested in how uncertain we are of these quantities, because the resulting phased image must reflect these uncertainties.

Figure 27.1: Nonlinear Phasing Example

(A) Linear Phases, the Real image

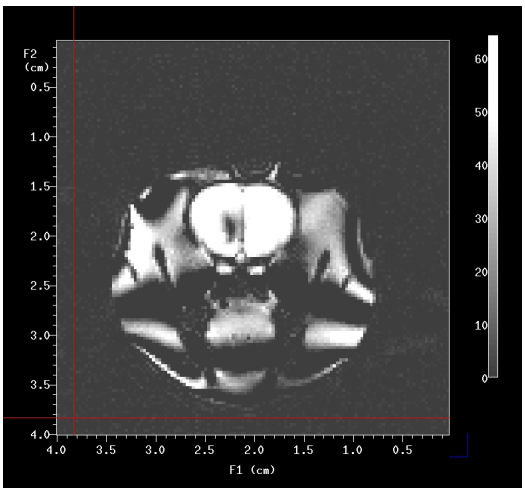

(B) Linear Phases, the Imaginary image

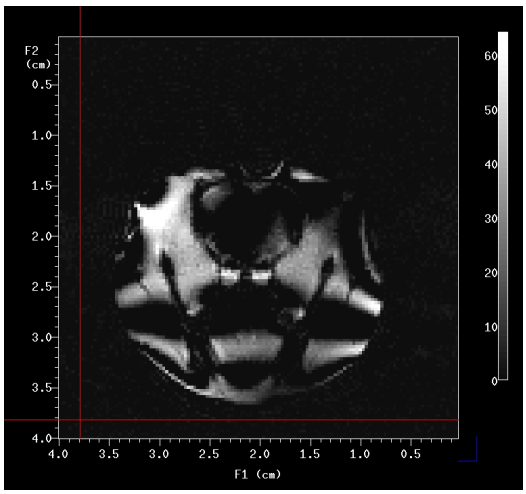

(C) Non-Linear Phases, the Real image

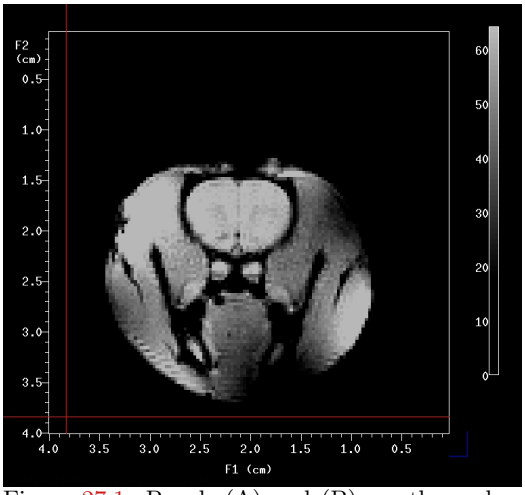

(D) Non-Linear Phases, the Imaginary image

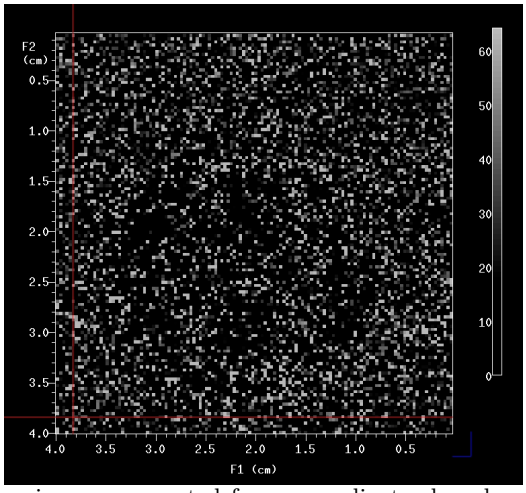

Figure 27.1: Panels (A) and (B) are the real and imaginary images generated from a gradient echo when the linear phasing algorithm is used. Note that the imaginary image, panel (B), still has a strong signal. This signal oscillates positive and negative in both the real and imaginary images. Panel (C) is the real image generated by the nonlinear phasing algorithm. The imaginary image (D) is essentially noise. If you compute the standard deviation of the noise from a section of the real and imaginary images you find they are essentially identical; indicating that the image is almost perfectly phased.

If d represents a complex image pixel value, then the model for any given pixel is

$$d = A \exp\{-\mathrm{i}\theta\} + n \tag{27.1}$$

where A is the amplitude of the image and θ is the phase. The quantity n represents the noise, and in this calculation we will assume the standard deviation of the noise, σ, is known. Separating the real and imaginary parts of this signal one has

$$d_R = A\cos(\theta) + n_R \tag{27.2}$$

for the real channel and

$$d_I = -A\sin(\theta) + n_I \tag{27.3}$$

for the imaginary channel, where d_R and d_R represent the real and imaginary pixel values and n_R and n_I represent the real and imaginary noise values. In the calculations which follow it will be assumed that the standard deviation of the noise is the same in both the real and imaginary channels and that the noise values are the same over the entire image.

27.2 The Bayesian Calculations

The Bayesian calculation consists of applying Bayes' theorem

$$P(A\theta|\sigma d_R d_I I) = \frac{P(A\theta|\sigma I)P(d_R d_I|\sigma A\theta I)}{P(d_R d_I|\sigma I)} \tag{27.4}$$

where $P(A\theta|\sigma dI)$ is the joint posterior probability for the parameters given the noise standard deviation, the data and the prior information I. The joint prior probability for the parameters, $P(A\theta|\sigma I)$, represents what was known about these parameters before the data were acquired. The direct probability for the data, $P(d_R d_I|\sigma A\theta I)$, is essentially the likelihood function and $P(d_R d_I|\sigma I)$ is a normalization constant. If we normalize this probability density function at the end of the calculation and factor the joint prior probability for the parameters, one obtains

$$P(A\theta|\sigma dI) \propto P(A|I)P(\theta|I)P(d|A\theta\sigma I) \tag{27.5}$$

as the joint posterior probability for the parameters.

In this calculation we will assign independent prior probabilities for the amplitude and Phase. And the likelihood will be assigned using a Gaussian prior probability. By definition the amplitude should be positive, but we do not wish to insert a hard lower bound on the amplitude. The reason for this is that in this analysis we are not doing a model selection calculation; rather we are doing a parameter estimation calculation. If we were doing a model selection calculation, then we could select between Eq. (27.1) and the "no signal" model. If we had done that then a hard cutoff would have worked fine as the prior probability. In regions were there is no signal, we would just get noise, and in regions where the signal is large we would get a properly phased signal. However, if we are doing parameter estimation, then a hard lower bound will necessarily force the real image to be positive, and so put a constant offset into the image: exactly the same thing that happens when one uses and absolute image. Consequently, we will use a prior that strongly suggests the amplitude

should be positive:

$$P(A|\sigma I) \propto \begin{cases} \exp\left[-\dfrac{A^2}{2\sigma^2}\right] & \text{if } A < -3\sigma \\ \exp\left[-\dfrac{A^2}{2\delta^2}\right] & \text{otherwise} \end{cases} \tag{27.6}$$

where δ is one half the maximum intensity in the image. So this prior expresses the belief that the amplitude should be small rather than large. Around zero this prior has almost no effect on negative amplitudes until the amplitude become more negative than three noise standard deviations, then suddenly this prior expresses a rather strong belief that the amplitude should be closer to zero. So small negative values are allowed, provided they are small enough not to protrude above the noise floor.

The prior probability for the phase is also assigned using a Gaussian prior probability of the form:

$$P(\theta|I) \propto \exp\left\{-\frac{\theta^2}{2 \times 2^2}\right\}. \tag{27.7}$$

This prior expresses a slight belief that the phase should be zero. The reason for this is simply that noise does not really have a phase, and so the phase should be zero. Any data item having even a small significant amplitude will quickly override this prior.

The likelihood, $P(d_R d_I|A\theta\sigma I)$ was assigned using a Gaussian given by

$$P(d_R d_I|A\theta\sigma I) \propto \exp\left\{-\frac{Q}{2\sigma^2}\right\} \tag{27.8}$$

where

$$Q \equiv [d_R - A\cos(\theta)]^2 + [d_I + A\sin(\theta)]^2. \tag{27.9}$$

In the program that implements the calculation, the noise standard deviation σ must be determined. There are many ways this might be done, but whatever is done, it must be general enough to work on any image. If you examine the output from the linear phasing routine, Fig. 27.1 panels (A) and (B), you will note that in small patches of the image, say 3×3 pixels, the signal in the real and imaginary channels are roughly constant; different constants in the real and imaginary, but constant nonetheless. If you postulate a model that is a constant in this small region and then compare the constant model to the "no signal" model, one can compute the posterior probability for these two models. If there is no signal present, then that region can be used to compute the noise standard deviation. By going over the entire image using a 3×3 set on pixels one can quickly get a very accurate estimate of the noise standard deviation by using only pixels for which the probability for no signal is much greater that the probability for the constant model.

The Bayesian calculations are implemented using Markov chain Monte Carlo, without simulated annealing. The Markov chain has Eq. (27.5) as its target distribution, using Eqs. (27.6,27.7) as the prior probabilities and Eq.(27.8) as the direct probability. The calculations are implemented in parallel, with parallelization occurring at the pixel level. Consequently, it 32 processors are available then 32 pixels are processed at one time. The simulations are initialized using the maximum likelihood estimated of both the amplitude and phase. Consequently, these simulations start very near the maximum of the joint posterior probability and all that is necessary is to run the simulations long enough for them to reach equilibrium.

In most Markov chain Monte Carlo simulations, it is the means and standard deviations of the parameter samples that are output. If we had used the mean phases to generate the output image, we would almost certainly get the maximum of the direct probability in regions were there is a signal, and, consequently, the output would essentially be an absolute value spectrum. However, we are not are not trying to estimate the amplitudes and phases, we are trying to phase an image. In the Markov chain Monte Carlo simulations each of the samples from the simulations are characteristic of the phase and amplitude supported by the data. Consequently, we randomly take one phase from one of the Markov chain Monte Carlo simulations and use that phase to produce an absorption mode pixel. This process is repeated for each pixel, giving an absorption model image. Figure 27.1 panels (C) and (D) are the real and imaginary parts of a gradient echo image that was phased using this procedure. Note that the real image (C) contains the fully phased image, plus noise; while the imaginary image (D) contains only noise. If one computes the noise standard deviation for these two images one finds essentially the same value in both real and imaginary images, and this value is the same as what is found in both panels (A) and (B), the real and imaginary parts of the linearly phased image; so this procedure has moved the positive intensity to the real channel and left the noise behind.

27.3 The Interfaces To The Nonlinear Phasing Routine

The interfaces to the Nonlinear Phasing package are shown in Fig. 27.2. To use this package you must:

- Run the linear phasing algorithm and have that package write both the imaginary and real FDF images.
- Select the type of processing:
  - **All**: all of images are to be phased separately.
  - **One**: only the currently displayed image is to be phased.
  - **Common**: the phase from the currently displayed image are to be computed, and those phases are then used on all of the images.
- Indicate if the imaginary images are to be written, the default is not to write these images.
- Indicate if the Ascii image are to be written, the default is not to write these images.

The remaining widgets on this interface are used to view the outputs and to indicate where the analysis is to be run. These widgets are pretty standard and we do not discuss them further. If you need to know more about the function of these widgets activate the help button and then activate the widget in question.

Figure 27.2: The Interface To The Nonlinear Phasing Package

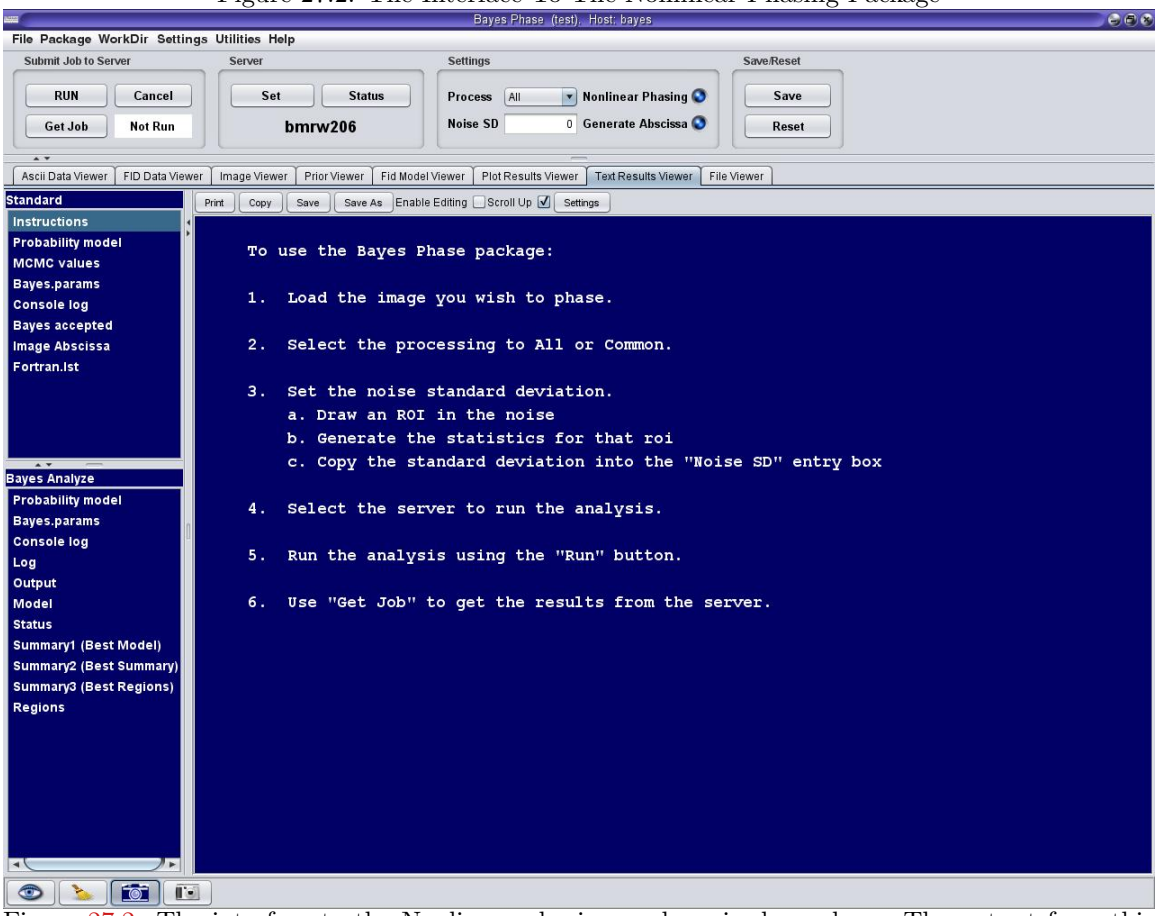

Figure 27.2: The interface to the Nonlinear phasing package is shown here. The output from this package is the phased real and imaginary parts of the input image. These images, usually just the real image, can be used in other analysis such as inversion recovery and diffusion tensor packages.

Bibliography

[1] Rev. Thomas Bayes (1763), "An Essay Toward Solving a Problem in the Doctrine of Chances," *Philos. Trans. R. Soc. London*, **53,** pp. 370-418; reprinted in *Biometrika*, **45**, pp. 293-315 (1958), and *Facsimiles of Two Papers by Bayes,* with commentary by W. Edwards Deming, New York, Hafner, 1963.

[2] G. Larry Bretthorst (1988), "Bayesian Spectrum Analysis and Parameter Estimation," in *Lecture Notes in Statistics,* **48**, J. Berger, S. Fienberg, J. Gani, K. Krickenberg, and B. Singer (eds), Springer-Verlag, New York, New York.

[3] G. Larry Bretthorst (1990), "An Introduction to Parameter Estimation Using Bayesian Probability Theory," in *Maximum Entropy and Bayesian Methods,* Dartmouth College 1989, P. Fougère *ed.,* pp. 53-79, Kluwer Academic Publishers, Dordrecht the Netherlands.

[4] G. Larry Bretthorst (1990), "Bayesian Analysis I. Parameter Estimation Using Quadrature NMR Models" *J. Magn. Reson.*, **88**, pp. 533-551.

[5] G. Larry Bretthorst (1990), "Bayesian Analysis II. Signal Detection And Model Selection" *J. Magn. Reson.*, **88**, pp. 552-570.

[6] G. Larry Bretthorst (1990), "Bayesian Analysis III. Examples Relevant to NMR" *J. Magn. Reson.*, **88**, pp. 571-595.

[7] G. Larry Bretthorst (1991), "Bayesian Analysis. IV. Noise and Computing Time Considerations," *J. Magn. Reson.*, **93**, pp. 369-394.

[8] G. Larry Bretthorst (1992), "Bayesian Analysis. V. Amplitude Estimation for Multiple Well-Separated Sinusoids," *J. Magn. Reson.*, **98**, pp. 501-523.

[9] G. Larry Bretthorst (1992), "Estimating The Ratio Of Two Amplitudes In Nuclear Magnetic Resonance Data," in *Maximum Entropy and Bayesian Methods,* C. R. Smith *et al.* (eds.), pp. 67-77, Kluwer Academic Publishers, the Netherlands.

[10] G. Larry Bretthorst (1993), "On The Difference In Means," in Physics & Probability Essays in honor of Edwin T. Jaynes, W. T. Grandy and P. W. Milonni (eds.), pp. 177-194, Cambridge University Press, England.

[11] G. Larry Bretthorst (1996), "An Introduction To Model Selection Using Bayesian Probability Theory," in *Maximum Entropy and Bayesian Methods*, G. R. Heidbreder, ed., pp. 1-42, Kluwer Academic Publishers, Printed in the Netherlands.

[12] G. Larry Bretthorst (1999), "The Near-Irrelevance of Sampling Frequency Distributions," in *Maximum Entropy and Bayesian Methods,* W. von der Linden *et al.* (eds.), pp. 21-46, Kluwer Academic Publishers, the Netherlands.

[13] G. Larry Bretthorst (2001), "Nonuniform Sampling: Bandwidth and Aliasing," in *Maximum Entropy and Bayesian Methods in Science and Engineering,* Joshua Rychert, Gary Erickson and C. Ray Smith *eds.*, pp. 1-28, American Institute of Physics, USA.

[14] G. Larry Bretthorst, Christopher D. Kroenke, and Jeffrey J. Neil (2004), "Characterizing Water Diffusion In Fixed Baboon Brain," in Bayesian Inference And Maximum Entropy Methods In Science And Engineering, Rainer Fischer, Roland Preuss and Udo von Toussaint *eds.*, AIP conference Proceedings, **735**, pp. 3-15.

[15] G. Larry Bretthorst, William C. Hutton, Joel R. Garbow, and Joseph J.H. Ackerman (2005), "Exponential parameter estimation (in NMR) using Bayesian probability theory," *Concepts in Magnetic Resonance*, 27A, Issue 2, pp. 55-63.

[16] G. Larry Bretthorst, William C. Hutton, Joel R. Garbow, and Joseph J. H. Ackerman (2005), "Exponential model selection (in NMR) using Bayesian probability theory," *Concepts in Magnetic Resonance*, 27A, Issue 2, pp. 64-72.

[17] G. Larry Bretthorst, William C. Hutton, Joel R. Garbow, and Joseph J.H. Ackerman (2005), "How accurately can parameters from exponential models be estimated? A Bayesian view," *Concepts in Magnetic Resonance*, 27A, Issue 2, pp. 73-83.

[18] G. Larry Bretthorst, W. C. Hutton, J. R. Garbow, and Joseph J. H. Ackerman (2008), "High Dynamic Range MRS Time-Domain Signal Analysis," *Magn. Reson. in Med.*, **62**, pp. 1026-1035.

[19] V. Chandramouli, K. Ekberg, W. C. Schumann, S. C. Kalhan, J. Wahren, and B. R. Landau (1997), "Quantifying gluconeogenesis during fasting," *American Journal of Physiology*, **273**, pp. H1209-H1215.

[20] R. T. Cox (1961), "The Algebra of Probable Inference," Johns Hopkins Univ. Press, Baltimore.

[21] André d'Avignon, G. Larry Bretthorst, Marilyn Emerson Holtzer, and Alfred Holtzer (1998), "Site-Specific Thermodynamics and Kinetics of a Coiled-Coil Transition by Spin Inversion Transfer NMR," *Biophysical Journal*, **74**, pp. 3190-3197.

[22] André d'Avignon, G. Larry Bretthorst, Marilyn Emerson Holtzer, and Alfred Holtzer (1999), "Thermodynamics and Kinetics of a Folded-Folded Transition at Valine-9 of a GCN4-Like Leucine Zipper," *Biophysical Journal*, **76**, pp. 2752-2759.

[23] David Freedman, and Persi Diaconis (1981), "On the histogram as a density estimator: L_2 theory," *Zeitschrift f¨r Wahrscheinlichkeitstheorie und verwandte Gebiete*, **57**, 4, pp. 453-476.

[24] W. R. Gilks, S. Richardson, and D. J. Spiegelhalter (1996), "Markov Chain Monte Carlo in Practice," Chapman & Hall, London.

[25] Paul M. Goggans, and Ying Chi (2004), "Using Thermodynamic Integration to Calculate the Posterior Probability in Bayesian Model Selection Problems," in *Bayesian Inference and Maximum Entropy Methods in Science and Engineering: 23rd International Workshop*, **707**, pp. 59-66.

[26] Marilyn Emerson Holtzer, G. Larry Bretthorst, D. André d'Avignon, Ruth Hogue Angelette, Lisa Mints, and Alfred Holtzer (2001), "Temperature Dependence of the Folding and Unfolding Kinetics of the GCN4 Leucine Lipper via 13C alpha-NMR," *Biophysical Journal*, **80**, pp. 939-951.

[27] E. T. Jaynes (1968), "Prior Probabilities," *IEEE Transactions on Systems Science and Cybernetics*, SSC-4, pp. 227-241; reprinted in [30].

[28] E. T. Jaynes (1978), "Where Do We Stand On Maximum Entropy?" in *The Maximum Entropy Formalism*, R. D. Levine and M. Tribus *Eds.*, pp. 15-118, Cambridge: MIT Press, Reprinted in [30].

[29] E. T. Jaynes (1980), "Marginalization and Prior Probabilities," in *Bayesian Analysis in Econometrics and Statistics*, A. Zellner *ed.,* North-Holland Publishing Company, Amsterdam; reprinted in [30].

[30] E. T. Jaynes (1983), "Papers on Probability, Statistics and Statistical Physics," a reprint collection, D. Reidel, Dordrecht the Netherlands; second edition Kluwer Academic Publishers, Dordrecht the Netherlands, 1989.

[31] E. T. Jaynes (1957), "How Does the Brain do Plausible Reasoning?" unpublished Stanford University Microwave Laboratory Report No. 421; reprinted in *Maximum-Entropy and Bayesian Methods in Science and Engineering* **1,** pp. 1-24, G. J. Erickson and C. R. Smith *Eds.,* 1988.

[32] E. T. Jaynes (2003), "Probability Theory—The Logic of Science," edited by G. Larry Bretthorst, Cambridge University Press, Cambridge UK.

[33] Sir Harold Jeffreys (1939), "Theory of Probability," Oxford Univ. Press, London; Later editions, 1948, 1961.

[34] John G. Jones, Michael A. Solomon, Suzanne M. Cole, A. Dean Sherry, and Craig R. Malloy (2001) "An integrated ^{2}H and ^{13}C NMR study of gluconeogenesis and TCA cycle flux in humans," *American Journal of Physiology, Endocrinology, and Metabolism,* **281,** pp. H848-H856.

[35] John Kotyk, N. G. Hoffman, W. C. Hutton, G. Larry Bretthorst, and J. J. H. Ackerman (1992), "Comparison of Fourier and Bayesian Analysis of NMR Signals. I. Well-Separated Resonances (The Single-Frequency Case)," *J. Magn. Reson.*, **98**, pp. 483–500.

[36] Pierre Simon Laplace (1814), "A Philosophical Essay on Probabilities," John Wiley & Sons, London, Chapman & Hall, Limited 1902. Translated from the 6th edition by F. W. Truscott and F. L. Emory.

[37] N. Lartillot, and H. Philippe (2006), "Computing Bayes Factors Using Thermodynamic Integration," *Systematic Biology*, **55** (2), pp. 195-207.

[38] D. Le Bihan, and E. Breton (1985), "Imagerie de diffusion in-vivo par rsonance," Comptes rendus de l'Acadmie des Sciences (Paris), **301** (15), pp. 1109-1112.

[39] N. R. Lomb (1976), "Least-Squares Frequency Analysis of Unevenly Spaced Data," *Astrophysical and Space Science*, **39**, pp. 447-462.

[40] T. J. Loredo (1990), "From Laplace To SN 1987A: Bayesian Inference In Astrophysics," in *Maximum Entropy and Bayesian Methods,* P. F. Fougere (ed), Kluwer Academic Publishers, Dordrecht, The Netherlands.

[41] Craig R. Malloy, A. Dean Sherry, and Mark Jeffrey (1988), "Evaluation of Carbon Flux and Substrate Selection through Alternate Pathways Involving the Citric Acid Cycle of the Heart by 13C NMR Spectroscopy," *Journal of Biological Chemistry*, **263** (15), pp. 6964-6971.

[42] Craig R. Malloy, Dean Sherry, and Mark Jeffrey (1990), "Analysis of tricarboxylic acid cycle of the heart using ^{13}C isotope isomers," *American Journal of Physiology*, **259**, pp. H987-H995.

[43] Lawrence R. Mead and Nikos Papanicolaou, "Maximum entropy in the problem of moments," *J. Math. Phys.* **25**, 2404–2417 (1984).

[44] K. Merboldt, Wolfgang Hanicke, and Jens Frahm (1969), "Self-diffusion NMR imaging using stimulated echoes," Journal of Magnetic Resonance, **64** (3), pp. 479-486.

[45] Nicholas Metropolis, Arianna W. Rosenbluth, Marshall N. Rosenbluth, Augusta H. Teller, and Edward Teller (1953), "Equation of State Calculations by Fast Computing Machines," Journal of Chemical Physics. The previous link is to the Americain Institute of Physics and if you do not have access to Science Sitations you many not be able to retrieve this paper.

[46] Radford M. Neal (1993), "Probabilistic Inference Using Markov Chain Monte Carlo Methods," technical report CRG-TR-93-1, Dept. of Computer Science, University of Toronto.

[47] Jeffrey J. Neil, and G. Larry Bretthorst (1993), "On the Use of Bayesian Probability Theory for Analysis of Exponential Decay Data: An Example Taken from Intravoxel Incoherent Motion Experiments," *Magn. Reson. in Med.*, **29**, pp. 642–647.

[48] H. Nyquist (1924), "Certain Factors Affecting Telegraph Speed," *Bell System Technical Journal*, **3**, pp. 324-346.

[49] H. Nyquist (1928), "Certain Topics in Telegraph Transmission Theory," *Transactions AIEE*, **3**, pp. 617-644.

[50] William H. Press, Saul A. Teukolsky, William T. Vetterling and Brian P. Flannery (1992), "Numerical Recipes The Art of Scientific Computing Second Edition," Cambridge University Press, Cambridge UK.

[51] Emanuel Parzen (1962), "On Estimation of a Probability Density Function and Mode," *Annals of Mathematical Statistics* **33**, 1065–1076

[52] Karl Pearson (1895), "Contributions to the Mathematical Theory of Evolution. II. Skew Variation in Homogeneous Material," *Phil. Trans. R. Soc. A* **186**, 343–326.

[53] Murray Rosenblatt, "Remarks on Some Nonparametric Estimates of a Density Function," *Annals of Mathematical Statistics* **27**, 832–837 (1956).

[54] Jeffery D. Scargle (1981), "Studies in Astronomical Time Series Analysis I. Random Process In The Time Domain," *Astrophysical Journal Supplement Series*, **45**, pp. 1-71.

[55] Jeffery D. Scargle (1982), "Studies in Astronomical Time Series Analysis II. Statistical Aspects of Spectral Analysis of Unevenly Sampled Data," *Astrophysical Journal*, **263**, pp. 835-853.

[56] Jeffery D. Scargle (1989), "Studies in Astronomical Time Series Analysis. III. Fourier Transforms, Autocorrelation Functions, and Cross-correlation Functions of Unevenly Spaced Data," *Astrophysical Journal*, **343**, pp. 874-887.

[57] Arthur Schuster (1905), "The Periodogram and its Optical Analogy," *Proceedings of the Royal Society of London*, **77**, p. 136-140.

[58] Claude E. Shannon (1948), "A Mathematical Theory of Communication," *Bell Syst. Tech. J.*, **27**, pp. 379-423.

[59] John E. Shore, and Rodney W. Johnson (1981), "Properties of cross-entropy minimization," *IEEE Trans. on Information Theory*, **IT-27,** No. 4, pp. 472-482.

[60] John E. Shore and Rodney W. Johnson (1980), "Axiomatic derivation of the principle of maximum entropy and the principle of minimum cross-entropy," *IEEE Trans. on Information Theory*, **IT-26** (1), pp. 26-37.

[61] Devinderjit Sivia, and John Skilling (2006), "Data Analysis: A Bayesian Tutorial," Oxford University Press, USA.

[62] Edward O. Stejskal and Tanner, J. E. (1965), "Spin Diffusion Measurements: Spin Echoes in the Presence of a Time-Dependent Field Gradient." Journal of Chemical Physics, **42** (1), pp. 288-292.

[63] D. G. Taylor and Bushell, M. C. (1985), "The spatial mapping of translational diffusion coefficients by the NMR imaging technique," Physics in Medicine and Biology, **30** (4), pp. 345-349.

[64] Myron Tribus (1969), "Rational Descriptions, Decisions and Designs," Pergamon Press, Oxford.

[65] P. M. Woodward (1953), "Probability and Information Theory, with Applications to Radar," McGraw-Hill, N. Y. Second edition (1987); R. E. Krieger Pub. Co., Malabar, Florida.

[66] Arnold Zellner (1971), "An Introduction to Bayesian Inference in Econometrics," John Wiley and Sons, New York.

Index